

# GDNTT: an Area-Efficient Parallel NTT Accelerator Using Glitch-Driven Near-Memory Computing and Reconfigurable 10T SRAM

Hengyu Ding<sup>†</sup>, Houran Ji<sup>†</sup>, Jia Li, Jinhang Chen, Chiu-Wing Sham, *Senior Member, IEEE*, Yao Wang, *Member, IEEE*

**Abstract**—With the rapid advancement of quantum computing technology, post-quantum cryptography (PQC) has emerged as a pivotal direction for next-generation encryption standards. Among these, lattice-based cryptographic schemes rely heavily on the fast Number Theoretic Transform (NTT) over polynomial rings, whose performance directly determines encryption/decryption throughput and energy efficiency. However, existing software-based NTT implementations struggle to meet the real-time performance and low-power requirements of IoT and edge devices. To address this challenge, this paper proposes an area-efficient highly parallel NTT accelerator with glitch-driven near-memory computing (GDNTT). The design integrates a 10T SRAM for data storage, enabling flexible row/column data access and streamlining circuit mapping strategies. Furthermore, a glitch generator is incorporated into the near-memory computing unit, significantly reducing the latency of butterfly operations. Evaluation results show that the proposed NTT accelerator achieves a 1.5~28× improvement in throughput-per-area compared to the state-of-the-art.

**Index Terms**—Number theoretic transform (NTT), near-memory computing, glitch generator, SRAM

## I. INTRODUCTION

THE rise of quantum computing threatens traditional encryption methods. As a post-quantum candidate, lattice-based cryptography resists quantum attacks but faces efficiency bottlenecks in polynomial multiplication [1], [2]. To address this, the Number Theoretic Transform (NTT) and its inverse (INTT) are widely adopted to accelerate computations, though they remain the most time-consuming operations in hardware implementations. Thus, optimizing NTT/INTT accelerators has become a critical research focus.

NTT accelerator architectures can be broadly classified into two types: Von Neumann-based and in-memory/near-memory computing. The Von Neumann approach, with

its separate compute and memory units, faces significant data movement overhead, limiting latency and memory efficiency [3], [4], [5]. In-memory/near-memory computing integrates processing units within or near memory, reducing data transfer overhead and improving energy efficiency and performance. Nejatollahi et al. [6] proposed a processing-in-memory NTT architecture with fast in-memory multiplication and modulo operations. Li et al. [7] developed a near-memory data mapping technique to optimize butterfly operation storage and resolve data conflicts. Park et al. [8] implemented an RRAM-based CiM NTT accelerator using vector-matrix multiplication for maximal parallelism. Zhang et al. [9] proposed a fast in-SRAM NTT with optimized bit-parallel modular multiplication and shift operations. Zhang et al. [10] developed an NTT using hybrid redundant numbers for carry-free modular multiplication and optimized memory patterns. Pakala et al. [11] introduced the MBSNTT architecture, which combines multi-bit serial modular multiplication with in-memory computing for fully parallel NTT operations. We observe that most in-memory or near-memory computing NTT accelerators require significant memory overhead in exchange for highly parallelized processing. For example, the 1024-point NTT proposed in [12], based on the Von Neumann architecture, uses only 1024 bits of RAM. In contrast, the 1024-point in-memory computing NTT designed in [10] utilizes 61440 bits of SRAM, which is 60 times that of the former.

In this brief, we propose GD-NTT (Glitch-Driven NTT), a highly parallel accelerator architecture featuring low memory and area overhead. The 10T SRAM supports concurrent row-column access for efficient butterfly operand pairing, while the glitch-based clock division technique generates precise timing signals to reduce near-memory computation latency. This dual optimization minimizes memory usage and maximizes throughput. Experimental results show the NTT achieves 67.1 kNTT/s at 256-point with only 0.006 mm<sup>2</sup> area, providing 1.5~28× better throughput-per-area compared to the state-of-the-art.

## II. BACKGROUND

NTT is a variant of the Fast Fourier Transform (FFT) performed over finite fields. Compared to FFT, NTT operates in a finite field, avoiding the errors and complexity associated with floating-point operations. Its primary

This work was supported by the Science and Technology Project of Henan Province under Grant 232102211076. (*Corresponding author: Yao Wang*)

<sup>†</sup>These authors contributed equally to this work.

Hengyu Ding, Houran Ji, Jia Li, Jinhang Chen and Yao Wang are with the School of Electrical and Information Engineering, Zhengzhou University, Zhengzhou 450001, China (e-mail: ieyaowang@zzu.edu.cn).

Chiu-Wing Sham is with the School of Computer Science, University of Auckland, Auckland 1010, New Zealand.

function is to accelerate polynomial multiplication. The transformation converts the polynomial coefficients from the time domain to the frequency domain, reducing the computational complexity of polynomial multiplication from  $O(N^2)$  to  $O(N \log N)$ . NTT plays an important role in cryptography, particularly in PQC and fully homomorphic encryption (FHE). NTT's basic principle is to use primitive roots and unity roots on finite fields to achieve fast transforms. Given a finite field  $F_q$  (where  $q$  is a prime), and a primitive root  $\omega$  such that  $\omega^n \equiv 1 \pmod{q}$  and for all  $i < n$ ,  $\omega^i \pmod{q}$  is an  $n$ -th primitive root of unity, for a polynomial  $a(x) = \sum_{j=0}^{n-1} a_j x^j$ , its  $n$ -point NTT computation is given by

$$A_i = \sum_{j=0}^{n-1} a_j \omega^{ij} \pmod{q} \quad (i = 0, 1, \dots, n-1) \quad (1)$$

INTT recovers the original polynomial  $a(x)$  from  $A(x)$ , which can be expressed as

$$a_i = \frac{1}{n} \sum_{j=0}^{n-1} A_j \cdot \omega^{-ij} \quad (2)$$

In this brief, we focus on implementing NTT and INTT transformations using the Cooley-Tukey and Gentleman-Sande algorithms, respectively. The Cooley-Tukey method, as shown in Alg. 1, decomposes large-scale NTT operations into smaller sub-operations through multi-layer loops, processing each part iteratively. In each loop, the results of adjacent computations are combined through butterfly operations, enabling efficient parallel computation of all terms. When performing the INTT transformation, the Gentleman-Sande method uses similar butterfly operations to revert the point-value form back to polynomial coefficients, as shown in Alg. 2.

---

**Algorithm 1** NTT algorithm with Cooley-Tukey method

---

**Input:** Polynomial  $x$ , modulus  $q$ , length  $n$ , inverse twiddle factor  $\omega$

**Output:**  $X = NTT(x)$

```

1:  $\hat{\omega} \leftarrow \text{bit-reverse}(\omega)$ 
2: if  $n == 1$  then
3:   return  $a$ 
4: end if
5: for  $i = 1; i < \log_2 n; i = i + 1$  do
6:    $m \leftarrow 2^i$ 
7:   for  $j = 0; j < (m/2); j = j + 1$  do
8:     for  $k = 0; k < (n/m); k = k + 1$  do
9:        $t \leftarrow x[k + 2 * j * (n/m)]$ 
10:       $u \leftarrow \hat{\omega}^j * x[k + 2 * (j + 1) * (n/m)] \pmod{q}$ 
11:       $X[k + 2 * j * (n/m)] \leftarrow (t + u) \pmod{q}$ 
12:       $X[k + (2j + 1) * (n/m)] \leftarrow (t - u) \pmod{q}$ 
13:     end for
14:   end for
15: end for

```

---



---

**Algorithm 2** INTT algorithm with Gentleman-Sande method

---

**Input:** Polynomial  $X$ , modulus  $q$ , length  $n$ , inverse twiddle factor  $\omega^{-1}$

**Output:**  $x = INTT(X)$

```

1:  $\hat{\omega}^{-1} \leftarrow \text{bit-reverse}(\omega^{-1})$ 
2:  $\hat{X} \leftarrow \text{bit-reverse}(X)$ 
3: for  $i = 1; i < \log_2 n; i = i + 1$  do
4:    $m \leftarrow 2^i$ 
5:   for  $j = 0; j < (n/m); j = j + 1$  do
6:     for  $k = 0; k < m/2; k = k + 1$  do
7:        $t \leftarrow \hat{X}[k + i * m]$ 
8:        $u \leftarrow \omega^{-j} * \hat{X}[k + j * m + m/2] \pmod{q}$ 
9:        $X[k + j * m] \leftarrow (t + u) \pmod{q}$ 
10:       $X[k + j * m + m/2] \leftarrow (t - u) \pmod{q}$ 
11:     end for
12:   end for
13: end for

```

---

### III. PROPOSED ARCHITECTURE

#### A. Overall Architecture

The overall architecture of the proposed NTT/INTT near-memory computing accelerator is illustrated in Fig. 1(a). The accelerator consists of modules such as the top level controller, glitch generator, SRAM array, near memory logic, and twiddle factor memory. The top level controller acts as the central control unit, overseeing the operation of all other components, including the SRAM array's row and column control, data retrieval, and writing back of results. The SRAM arrays, represented in blue, are used to store operands and intermediate results in two separate sets. The near memory logic units (highlighted in yellow) carry out computations close to the memory. These modules contain a butterfly operation unit that performs arithmetic operations, such as multiplication, and a twiddle factor memory that stores pre-computed rotation factors used in the butterfly operations. Furthermore, these near memory logic units enable data exchange between the two SRAM arrays, facilitating the point-wise multiplication of two data sets post-NTT computation. The glitch generator generates multiple narrow pulse-width signals with the same frequency as the main clock, used to synchronously drive row control, column control, and near-memory computing units, enabling the continuous execution of multi-step near-memory logic operations within a single clock cycle. Driven by a series of narrow pulse width signals generated by the glitch generator, we are able to complete SRAM data reading, near-memory computation, and storage of the computation results within a single clock cycle.

#### B. Design of 10T SRAM and Parallel Memory Access Scheme

In conventional vector computing, there is no logical operation between rows, that is, the rows are decoupled.

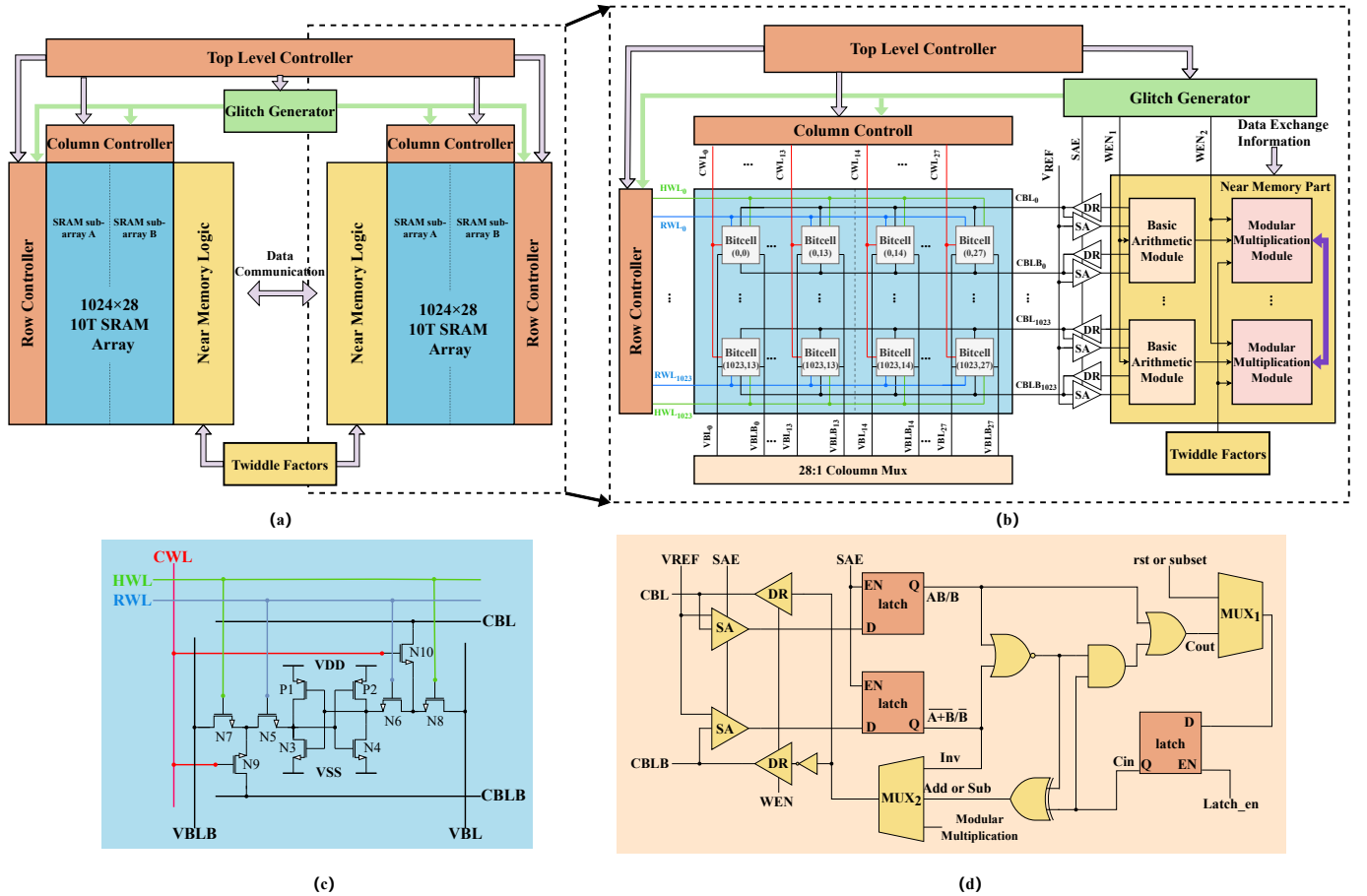


Fig. 1. (a) Overall architecture of the proposed NTT accelerator. (b) Detailed structure of the near-memory computation unit. (c) Structure of the proposed 10T SRAM bit-cell. (d) Structure of the basic arithmetic module.

However, in the NTT calculation process, there is a coupling relationship between rows. Conventional 8T SRAM architectures rely on column word lines (CWL) to control the access of each bit cell in a column. However, precise row-level control is unachievable with this configuration. To address this limitation, we designed a 10T SRAM bit cell, shown in Fig. 1(c).

In this design, when performing read/write operations via VBL and VBLB, both RWL and HWL are set to high while CWL remains low. This configuration turns on transistors N5, N6, N7, and N8, connecting VBL and VBLB to the bit cell while isolating CBL and CBLB through N9 and N10. In this configuration, the SRAM bit cell can perform read/write operations on the near-memory computing unit via the VBL and VBLB lines. Conversely, when accessing the CBL and CBLB lines, RWL and CWL are pulled to high to achieve precise bit cell control, while HWL is set to low. This activates N5, N6, N8, and N9, linking CBL and CBLB to the circuit while isolating VBL and VBLB via N7 and N8. In this case, the SRAM bit cell is connected to the input/output interface of the NTT accelerator through a column MUX. This approach allows dynamic row selection during data migration, thereby achieving precise matching of butterfly

operation data pairs across different computational stages.

### C. Near-Memory Computation

Our NTT/INTT operations are based on the Cooley-Tukey algorithm and the Gentleman-Sande algorithm, implementing the conventional data flow of NTT/INTT computations. Fig. 2 provides an illustrative example of the computational process for a single-stage butterfly operation in a 4-point NTT. The mapping of data between butterfly operation stages is achieved through two data exchanges in *Stage1* and *Stage2*. In *Stage1*, we perform data migration of the original data to enable direct parallel computation. The process begins by reading corresponding data according to the number of butterfly stages. Once data is read from the SRAM via CBL and CBLB lines, it is amplified by sense amplifiers and fed into the near-memory computation unit. Specifically,  $a_0$  and  $a_1$  are sequentially loaded into registers in the near-memory computation unit before data transfer. The purple lines in Fig. 1(b) represent the data transmission channels between different near-memory computing units. Through these data channels,  $a_0$  and  $a_1$  are transmitted to another set of near-memory computing units, and then the data from the two sets of near-memory computing units are written in parallel into

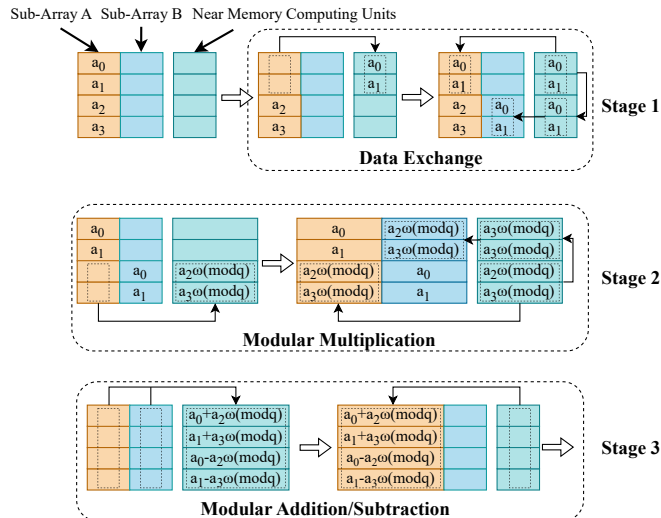


Fig. 2. Detailed NTT calculation flow.

SRAM sub-arrays A and B, respectively. Since the original data in the SRAM sub-array A will disappear after read operations, a copy of the original data must be rewritten back to the SRAM sub-array A. At this stage, we have successfully completed half of the data exchange process.

The modular multiplication of NTT is demonstrated in *Stage2* of Fig. 2. We employ the standard Barrett modular multiplication method.  $a_2$  and  $a_3$  are read in parallel from the SRAM array and carries out modular multiplication operations in near-memory computing units. After completing the modular multiplication, the results are written back to the remaining blank SRAM arrays in sub-array A and B using the identical data exchange methodology implemented in Stage 1.

*Stage3* demonstrates the modular addition/subtraction operations. The detailed data transfer mechanism will be systematically elaborated in the subsequent subsection. Fig. 1(d) illustrates the internal structure of the basic arithmetic module, which carries out addition and subtraction operations. When executing addition, operands  $A$  and  $B$  are fed into latches via CBL and CBLB, where XOR logic computes  $A \oplus B$ . Carry information is propagated through MUX1, which selects either an initial reset value or the previous stage's carry-out value. The sum is computed iteratively and stored back in SRAM. For subtraction,  $B$  is first inverted, then  $A$  and the inverted  $B$  carry out an addition operation with an initial carry-in value of 1. The MUX2 determines whether the output is from addition/subtraction or the modular multiplication module. Upon completion of Stage 3, the processed data is concurrently written into SRAM sub-array A through parallel write operations, where it is retained for subsequent computational phases.

#### D. Glitch-driven High-speed Butterfly Operation

The Glitch Generator, as shown in the top-left corner of Fig. 3, produces multiple narrow pulse-width signals within a single clock cycle, primarily used for controlling

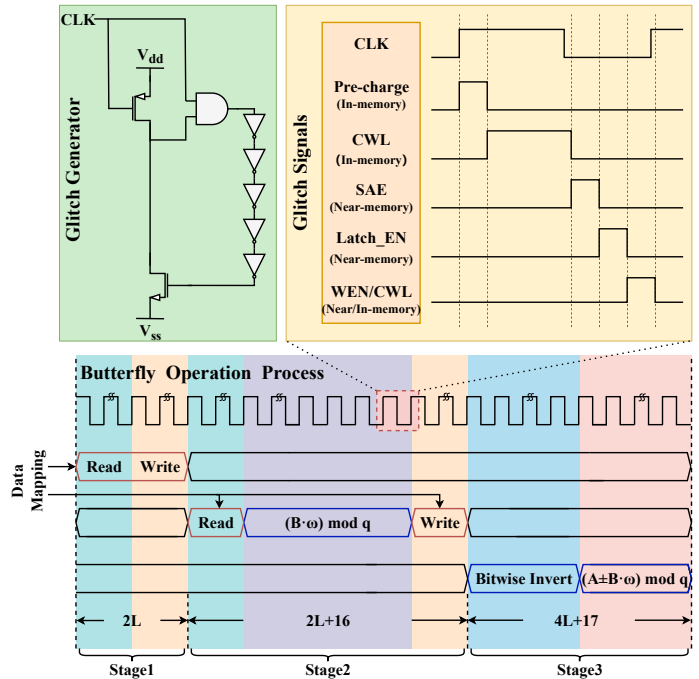


Fig. 3. Schematic of the glitch generator and critical timing waveforms for NTT operations.

SRAM or near-memory computing units. Under the control of the glitch signals, near-memory computing units perform consecutive operations within a single clock cycle, significantly accelerating the speed of butterfly operations. Fig. 3 illustrates the detailed schematic diagram of the glitch generator with its corresponding waveform, along with the timing diagram of a single-stage butterfly operation. The data mapping is completed through two data exchanges in *Stage1* and *Stage2*. Note that a read or write operation requires  $L$  cycles for  $L$  bits of data. The modular multiplication takes 16 cycles. Bit reversal and addition/subtraction operations allow single-bit data to be read and processed within one cycle. During the implementation of addition/subtraction operations, the data designated for subtraction is first fully read out, subjected to bitwise inversion, and rewritten to the SRAM arrays. Subsequently, a parallel readout of all row data is executed to perform modular addition operations, thereby obtaining the final computational results. The addition/subtraction steps require almost no additional cycles except for the final modular operation. *Stage3* completes in  $4L + 17$  cycles.

## IV. RESULTS AND DISCUSSION

We evaluate the proposed NTT in a 28 nm CMOS process. Table I provides the results and comparisons of recent NTT designs and this work. In the case of  $N = 256$ , the throughput of the proposed NTT accelerator reaches 67.1 kNTT/s, with a minimal area overhead of only  $0.006 m^2$ , achieving the highest throughput-per-area ( $11183.3 \text{ KNTT/s/mm}^2$ ). In comparison, the proposed

TABLE I  
COMPARISON WITH STATE-OF-THE-ART NTT ACCELERATORS

Design	Type	N	Freq (MHz)	Bit width	Tput. (kNTT/s)	Latency ( $\mu$ s)	Energy (nJ/NTT)	Area (mm <sup>2</sup> )	Tput./area (kNTT/s/mm <sup>2</sup> )
This work (28nm)	SRAM CIM	256	176	14	67.1	14.9	622	0.006	11183.3
		512	163	14	51.5	19.4	714	0.011	4681.8
		1024	148	14	37.3	26.8	766	0.021	1776.2
TVLSI 2025 (28nm <sup>a</sup> ) [11]	SRAM CIM	1024	167	32	62	16.1	126	0.154	403
DAC 2023 (28nm <sup>a</sup> ) [9]	SRAM CIM	256	3800	16	26	38.5	13	0.024	1082
TVLSI 2022 (28nm <sup>a</sup> ) [7]	SRAM PIM	1024	151	14	80	12.5	93	0.067	1195
MICRO 2021 (28nm <sup>a</sup> ) [14]	Pipelined	8K	2000	128	36k	0.028	1.24M	68.139	524
DAC 2020 (28nm <sup>a</sup> ) [6]	ReRAM PIM	256	909	16	23.4	42.7	1007	0.059 <sup>b</sup>	397
ICASSP 2020 (28nm <sup>a</sup> ) [13]	FPGA	1024	182.98	16	14	71.3	6135	-	-
CICC 2018 (28nm <sup>a</sup> ) [15]	ASIC	256	267	14	2.7k	0.4	17	0.685 <sup>b</sup>	3910

**Notes:** a. The process nodes are normalized to 28nm CMOS Process for an apples-to-apples comparison with GD-NTT.  
b. The areas are estimated by referring to work [9].

structure demonstrates  $1.6 \times / 2.9 \times / 2.7 \times$  higher throughput than those of [9], [6] and [13], respectively, while achieving  $4 \times / 10 \times$  area reduction compared to [9] and [6]. Although the NTT designs in [11], [7], [14], and [15] outperform the proposed structure in throughput, they require at least  $3.2 \times$  more area. This work demonstrates a balanced performance between throughput and area efficiency, providing  $1.5 \sim 28 \times$  better throughput-per-area compared to the state-of-the-art.

## V. CONCLUSION

This brief proposes a near-memory NTT accelerator that enhances polynomial multiplication for post-quantum cryptography. Our design combines reconfigurable SRAM, glitch-driven execution, and near-memory computing to optimize throughput and efficiency. The architecture overcomes traditional memory bottlenecks and latency issues. Evaluation results show that GD-NTT can achieve a significant improvement in throughput-per-area (up to  $28 \times$ ) over the latest ASIC and in-memory designs, offering an efficient solution for edge devices and advancing cryptographic hardware research.

## REFERENCES

- [1] A. Aysu, C. Patterson, and P. Schaumont, "Low-cost and area-efficient FPGA implementations of lattice-based cryptography," in *Proc. IEEE Int. Symp. Hardware-Oriented Security and Trust (HOST)*, 2013, pp. 81–86.
- [2] P. He, Y. Tu, J. Xie, and H. S. Jacinto, "KINA: Karatsuba initiated novel accelerator for ring-binary-lwe (RBLWE)-based post-quantum cryptography," *IEEE Trans. Very Large Scale Integr. (VLSI) Syst.*, vol. 31, no. 10, pp. 1551–1564, 2023.
- [3] C. Zhang, D. Liu, X. Liu, X. Zou, G. Niu, B. Liu, and Q. Jiang, "Towards efficient hardware implementation of NTT for KYBER ON FPGAs," in *Proc. IEEE Int. Symp. Circuits Syst. (ISCAS)*, 2021, pp. 1–5.
- [4] R. Paludo and L. Sousa, "NTT architecture for a linux-ready RISC-V fully-homomorphic encryption accelerator," *IEEE Trans. Circuits Syst. I, Reg. Pap.*, vol. 69, no. 7, pp. 2669–2682, 2022.
- [5] Z. Cheng, B. Zhang, and M. Pedram, "A high-performance, conflict-free memory-access architecture for modular polynomial multiplication," *IEEE Trans. Comput.-Aided Des. Integr. Circuits Syst.*, vol. 43, no. 2, pp. 492–505, 2024.
- [6] H. Nejatollahi, S. Gupta, M. Imani, T. S. Rosing, R. Cammarota, and N. Dutt, "CryptoPIM: In-memory acceleration for lattice-based cryptographic hardware," in *Proc. ACM/IEEE Design Autom. Conf. (DAC)*, 2020, pp. 1–6.
- [7] D. Li, A. Pakala, and K. Yang, "M<sub>ENTT</sub>: A compact and efficient processing-in-memory number theoretic transform (NTT) accelerator," *IEEE Trans. Very Large Scale Integr. (VLSI) Syst.*, vol. 30, no. 5, pp. 579–588, 2022.
- [8] Y. Park, Z. Wang, S. Yoo, and W. D. Lu, "RM-NTT: An RRAM-based compute-in-memory number theoretic transform accelerator," *IEEE J. Explor. Solid-State Comput. Devices Circuits*, vol. 8, no. 2, pp. 93–101, 2022.
- [9] J. Zhang, M. Imani, and E. Sadredini, "BP-NTT: Fast and compact in-sram number theoretic transform with bit-parallel modular multiplication," in *2023 60th ACM/IEEE Design Automation Conference (DAC)*, 2023, pp. 1–6.
- [10] X. Zhang, Y. Wei, M. Li, J. Tian, and Z. Wang, "HRCIM-NTT: An efficient compute-in-memory NTT accelerator with hybrid-redundant numbers," *IEEE Trans. Circuits Syst. I, Reg. Pap.*, vol. 72, no. 1, pp. 214–227, 2025.
- [11] A. Pakala, Z. Chen, and K. Yang, "MBSNTT: A highly parallel digital in-memory bit-serial number theoretic transform accelerator," *IEEE Transactions on Very Large Scale Integration (VLSI) Systems*, vol. 33, no. 2, pp. 537–545, 2025.
- [12] Y. Zhao, X. Liu, Y. Hu, and H. Xiao, "Design of an efficient NTT/INTT architecture with low-complex memory mapping scheme," *IEEE Trans. Circuits Syst. II, Exp. Briefs*, vol. 71, no. 1, pp. 400–404, 2024.
- [13] H. Nejatollahi, S. Shahhosseini, R. Cammarota, and N. Dutt, "Exploring energy efficient quantum-resistant signal processing using array processors," in *Proc. IEEE Int. Conf. Acoust. Speech Signal Process. (ICASSP)*, 2020, pp. 1539–1543.
- [14] N. Samardzic, A. Feldmann, A. Krastev, S. Devadas, R. Dreslinski, C. Peikert, and D. Sanchez, "F1: A fast and programmable accelerator for fully homomorphic encryption," in *Proc. IEEE/ACM Int. Symp. Microarchitecture (MICRO)*, 2021, p. 238–252.
- [15] S. Song, W. Tang, T. Chen, and Z. Zhang, "LEIA: A 2.05mm<sup>2</sup> 140mW lattice encryption instruction accelerator in 40nm

CMOS,” in *Proc. IEEE Custom Integr. Circuits Conf. (CICC)*, 2018, pp. 1–4.